Instrument Noise, Retrieval Issues or Geophysical Signal?

Peter Cornillon[1], Jörn Callis[2] & J. Xavier Prochaska[3]

[1]Graduate School of Oceanography, University of Rhode Island, Narragansett, RI 02882, USA
[2]California Institute of Technology, Pasadena, CA 91125, USA
[3]Department of Astronomy and Astrophysics, University of California, Santa Cruz, CA 95064, USA

May 24, 2021

Acknowledgments

- NASA grant # 80NSSC18K0837 via a subcontract from the Farallon Institute and
- X Prochaska received support from the University of California, Santa Cruz.

Outline

Machine Learning Used to Discover Anomalous SST Fields

- In an effort to find unusual SST fields, pointing to intriguing physical processes,

  We used a ML algorithm to examine a subset of the MODIS Aqua L2 dataset.

  - Period: 2003-2019.
  - Global.
  - Nighttime only.

- The $\approx 10^6$ resulting granules were produced by & obtained from the OBPG/GSFC.
- Our ML analysis & results are discussed in the previous presentation S2-ID-036 & in:

  Prochaska, J.X.; Cornillon, P.C.; Reiman, D.M.
  Deep Learning of Sea Surface Temperature Patterns to Identify Ocean Extremes
  Remote Sens. 2021, 13(4), 744; https://doi.org/10.3390/rs13040744.

- And will not be repeated here.
- However, the work described in this presentation is based on the same dataset.

OBPG - Ocean Biology Processing Group
GSFC - NASA's Goddard Space Flight Center
5-minute granule corresponds to the data collected by the data in 5 minutes.

Machine Learning Used to Discover Anomalous SST Fields

- In an effort to find unusual SST fields, pointing to intriguing physical processes,

  We used a ML algorithm to examine a subset of the MODIS Aqua L2 dataset.
  - Period: 2003-2019.
  - Global.
  - Nighttime only.
- The $\approx 10^6$ resulting granules were produced by & obtained from the OBPG/GSFC.
- Our ML analysis & results are discussed in the previous presentation S2-ID-036 & in:

  Prochaska, J.X.; Cornillon, P.C.; Reiman, D.M.
  Deep Learning of Sea Surface Temperature Patterns to Identify Ocean Extremes
  Remote Sens. 2021, 13(4), 744; https://doi.org/10.3390/rs13040744.
- And will not be repeated here.
- However, the work described in this presentation is based on the same dataset.

OBPG - Ocean Biology Processing Group
GSFC - NASA's Goddard Space Flight Center
5-minute granule corresponds to the data collected by the data in 5 minutes.

Machine Learning Used to Discover Anomalous SST Fields

- In an effort to find unusual SST fields, pointing to intriguing physical processes,

  We used a ML algorithm to examine a subset of the MODIS Aqua L2 dataset.

  - Period: 2003-2019.
  - Global.
  - Nighttime only.

- The $\approx 10^6$ resulting granules were produced by & obtained from the OBPG/GSFC.
- Our ML analysis & results are discussed in the previous presentation S2-ID-036 & in:

  Prochaska, J.X.; Cornillon, P.C.; Reiman, D.M.
  Deep Learning of Sea Surface Temperature Patterns to Identify Ocean Extremes
  Remote Sens. 2021, 13(4), 744; https://doi.org/10.3390/rs13040744.

- And will not be repeated here.
- However, the work described in this presentation is based on the same dataset.

OBPG - Ocean Biology Processing Group
GSFC - NASA's Goddard Space Flight Center
5-minute granule corresponds to the data collected by the data in 5 minutes.

Machine Learning Used to Discover Anomalous SST Fields

- In an effort to find unusual SST fields, pointing to intriguing physical processes,

  We used a ML algorithm to examine a subset of the MODIS Aqua L2 dataset.
  - Period: 2003-2019.
  - Global.
  - Nighttime only.
- The $\approx 10^6$ resulting granules were produced by & obtained from the OBPG/GSFC.
- Our ML analysis & results are discussed in the previous presentation S2-ID-036 & in:

  Prochaska, J.X.; Cornillon, P.C.; Reiman, D.M.
  Deep Learning of Sea Surface Temperature Patterns to Identify Ocean Extremes
  Remote Sens. 2021, 13(4), 744; https://doi.org/10.3390/rs13040744.
- And will not be repeated here.
- However, the work described in this presentation is based on the same dataset.

OBPG - Ocean Biology Processing Group
GSFC - NASA's Goddard Space Flight Center
5-minute granule corresponds to the data collected by the data in 5 minutes.

Machine Learning Used to Discover Anomalous SST Fields

- In an effort to find unusual SST fields, pointing to intriguing physical processes,

  We used a ML algorithm to examine a subset of the MODIS Aqua L2 dataset.
    - Period: 2003-2019.
    - Global.
    - Nighttime only.
- The $\approx 10^6$ resulting granules were produced by & obtained from the OBPG/GSFC.
- Our ML analysis & results are discussed in the previous presentation S2-ID-036 & in:

  Prochaska, J.X.; Cornillon, P.C.; Reiman, D.M.
  Deep Learning of Sea Surface Temperature Patterns to Identify Ocean Extremes
  Remote Sens. 2021, 13(4), 744; https://doi.org/10.3390/rs13040744.
- And will not be repeated here.
- However, the work described in this presentation is based on the same dataset.

OBPG - Ocean Biology Processing Group
GSFC - NASA's Goddard Space Flight Center
5-minute granule corresponds to the data collected by the data in 5 minutes.

Machine Learning Used to Discover Anomalous SST Fields

- In an effort to find unusual SST fields, pointing to intriguing physical processes,

  We used a ML algorithm to examine a subset of the MODIS Aqua L2 dataset.
  - Period: 2003-2019.
  - Global.
  - Nighttime only.
- The $\approx 10^6$ resulting granules were produced by & obtained from the OBPG/GSFC.
- Our ML analysis & results are discussed in the previous presentation S2-ID-036 & in:

  Prochaska, J.X.; Cornillon, P.C.; Reiman, D.M.
  Deep Learning of Sea Surface Temperature Patterns to Identify Ocean Extremes
  Remote Sens. 2021, 13(4), 744; https://doi.org/10.3390/rs13040744.
- And will not be repeated here.
- However, the work described in this presentation is based on the same dataset.

OBPG - Ocean Biology Processing Group
GSFC - NASA's Goddard Space Flight Center
5-minute granule corresponds to the data collected by the data in 5 minutes.

Our Approach

- As noted in S2-ID-036 we used 128×128 pixel samples extracted from the L2 fields:
  - We refer to these approximately 128×128 km^2 extractions as cutouts.
  - Cutouts were restricted to be:
    - >95% "clear",
    - Within 400 pixels of nadir, and
    - $< \approx 50\%$ overlap
  - Resulted in ≈12 million cutouts.
- In an attempt to find what the ML algorithm was keying on, we examined cutout:
  - Temperature range
  - Variance
  - Along-scan and along-track structure functions and
  - Along-scan and along-track power spectral densities (PSD).
- With some intriguing results for the latter.
- Specifically, we plotted the along-scan PSD for cutouts constrained to have:
  - $2.0 < T_{90} - T_{10} < 2.1K$ and
  - Log likelihood, determined by the ML algorithm (S2-ID-036) , > 194
- These constrains lead to spectra with about the same overall energy level

  Making it straightforward to compare them.

Our Approach

- As noted in S2-ID-036 we used 128×128 pixel samples extracted from the L2 fields:
  - We refer to these approximately 128×128 km^2 extractions as cutouts.
  - Cutouts were restricted to be:
    - $>95\%$ "clear",
    - Within 400 pixels of nadir, and
    - $<\approx 50\%$ overlap
  - Resulted in $\approx$12 million cutouts.
- In an attempt to find what the ML algorithm was keying on, we examined cutout:
  - Temperature range
  - Variance
  - Along-scan and along-track structure functions and
  - Along-scan and along-track power spectral densities (PSD).
- With some intriguing results for the latter.
- Specifically, we plotted the along-scan PSD for cutouts constrained to have:
  - $2.0 < T_{90} - T_{10} < 2.1K$ and
  - Log likelihood, determined by the ML algorithm (S2-ID-036) , > 194
- These constrains lead to spectra with about the same overall energy level

  Making it straightforward to compare them.

Our Approach

- As noted in S2-ID-036 we used 128×128 pixel samples extracted from the L2 fields:
  - We refer to these approximately 128×128 km^2 extractions as cutouts.
  - Cutouts were restricted to be:
    - $>$95% "clear",
    - Within 400 pixels of nadir, and
    - $<\approx$ 50% overlap
  - Resulted in ≈12 million cutouts.
- In an attempt to find what the ML algorithm was keying on, we examined cutout:
  - Temperature range
  - Variance
  - Along-scan and along-track structure functions and
  - Along-scan and along-track power spectral densities (PSD).
- With some intriguing results for the latter.
- Specifically, we plotted the along-scan PSD for cutouts constrained to have:
  - $2.0 < T_{90} - T_{10} < 2.1K$ and
  - Log likelihood, determined by the ML algorithm (S2-ID-036) , > 194
- These constrains lead to spectra with about the same overall energy level

  Making it straightforward to compare them.

Our Approach

- As noted in S2-ID-036 we used 128×128 pixel samples extracted from the L2 fields:
  - We refer to these approximately 128×128 km^2 extractions as cutouts.
  - Cutouts were restricted to be:
    - $>$95% “clear",
    - Within 400 pixels of nadir, and
    - $< \approx$ 50% overlap
  - Resulted in $\approx$12 million cutouts.
- In an attempt to find what the ML algorithm was keying on, we examined cutout:
  - Temperature range
  - Variance
  - Along-scan and along-track structure functions and
  - Along-scan and along-track power spectral densities (PSD).
- With some intriguing results for the latter.
- Specifically, we plotted the along-scan PSD for cutouts constrained to have:
  - $2.0 < T_{90} - T_{10} < 2.1K$ and
  - Log likelihood, determined by the ML algorithm (S2-ID-036) , > 194
- These constrains lead to spectra with about the same overall energy level

  Making it straightforward to compare them.

Our Approach

- As noted in S2-ID-036 we used 128×128 pixel samples extracted from the L2 fields:
  - We refer to these approximately 128×128 km^2 extractions as cutouts.
  - Cutouts were restricted to be:
    - $>$95% “clear",
    - Within 400 pixels of nadir, and
    - $<\approx$ 50% overlap
  - Resulted in ≈12 million cutouts.
- In an attempt to find what the ML algorithm was keying on, we examined cutout:
  - Temperature range
  - Variance
  - Along-scan and along-track structure functions and
  - Along-scan and along-track power spectral densities (PSD).
- With some intriguing results for the latter.
- Specifically, we plotted the along-scan PSD for cutouts constrained to have:
  - $2.0 < T_{90} - T_{10} < 2.1K$ and
  - Log likelihood, determined by the ML algorithm (S2-ID-036) , > 194
- These constrains lead to spectra with about the same overall energy level

  Making it straightforward to compare them.

Our Approach

- As noted in S2-ID-036 we used 128×128 pixel samples extracted from the L2 fields:
  - We refer to these approximately 128×128 km^2 extractions as cutouts.
  - Cutouts were restricted to be:
    - $>$95% “clear",
    - Within 400 pixels of nadir, and
    - $<\approx$ 50% overlap
  - Resulted in $\approx$12 million cutouts.
- In an attempt to find what the ML algorithm was keying on, we examined cutout:
  - Temperature range
  - Variance
  - Along-scan and along-track structure functions and
  - Along-scan and along-track power spectral densities (PSD).
- With some intriguing results for the latter.
- Specifically, we plotted the along-scan PSD for cutouts constrained to have:
  - $2.0 < T_{90} - T_{10} < 2.1K$ and
  - Log likelihood, determined by the ML algorithm (S2-ID-036) , > 194
- These constrains lead to spectra with about the same overall energy level

  Making it straightforward to compare them.

Our Approach

- As noted in S2-ID-036 we used 128$\times$128 pixel samples extracted from the L2 fields:
  - We refer to these approximately 128$\times$128 km^2 extractions as cutouts.
  - Cutouts were restricted to be:
    - $>$95% “clear",
    - Within 400 pixels of nadir, and
    - $<\approx$ 50% overlap
  - Resulted in $\approx$12 million cutouts.
- In an attempt to find what the ML algorithm was keying on, we examined cutout:
  - Temperature range
  - Variance
  - Along-scan and along-track structure functions and
  - Along-scan and along-track power spectral densities (PSD).
- With some intriguing results for the latter.
- Specifically, we plotted the along-scan PSD for cutouts constrained to have:
  - $2.0 < T_{90} - T_{10} < 2.1K$ and
  - Log likelihood, determined by the ML algorithm (S2-ID-036) , > 194
- These constrains lead to spectra with about the same overall energy level

  Making it straightforward to compare them.

Our Approach

- As noted in S2-ID-036 we used 128×128 pixel samples extracted from the L2 fields:
  - We refer to these approximately 128×128 km^2 extractions as cutouts.
  - Cutouts were restricted to be:
    - $>$95% “clear",
    - Within 400 pixels of nadir, and
    - $<\approx$ 50% overlap
  - Resulted in $\approx$12 million cutouts.
- In an attempt to find what the ML algorithm was keying on, we examined cutout:
  - Temperature range
  - Variance
  - Along-scan and along-track structure functions and
  - Along-scan and along-track power spectral densities (PSD).
- With some intriguing results for the latter.
- Specifically, we plotted the along-scan PSD for cutouts constrained to have:
  - $2.0 < T_{90} - T_{10} < 2.1K$ and
  - Log likelihood, determined by the ML algorithm (S2-ID-036) , > 194
- These constrains lead to spectra with about the same overall energy level

  Making it straightforward to compare them.

Our Approach

- As noted in S2-ID-036 we used 128×128 pixel samples extracted from the L2 fields:
  - We refer to these approximately 128×128 km^2 extractions as cutouts.
  - Cutouts were restricted to be:
    - $>$95% “clear",
    - Within 400 pixels of nadir, and
    - $<\approx$ 50% overlap
  - Resulted in $\approx$12 million cutouts.
- In an attempt to find what the ML algorithm was keying on, we examined cutout:
  - Temperature range
  - Variance
  - Along-scan and along-track structure functions and
  - Along-scan and along-track power spectral densities (PSD).
- With some intriguing results for the latter.
- Specifically, we plotted the along-scan PSD for cutouts constrained to have:
  - $2.0 < T_{90} - T_{10} < 2.1K$ and
  - Log likelihood, determined by the ML algorithm (S2-ID-036) , > 194
- These constrains lead to spectra with about the same overall energy level

  Making it straightforward to compare them.

Our Approach

- As noted in S2-ID-036 we used 128×128 pixel samples extracted from the L2 fields:
  - We refer to these approximately 128×128 km^2 extractions as cutouts.
  - Cutouts were restricted to be:
    - $>$95% “clear",
    - Within 400 pixels of nadir, and
    - $<\approx$ 50% overlap
  - Resulted in ≈12 million cutouts.
- In an attempt to find what the ML algorithm was keying on, we examined cutout:
  - Temperature range
  - Variance
  - Along-scan and along-track structure functions and
  - Along-scan and along-track power spectral densities (PSD).
- With some intriguing results for the latter.
- Specifically, we plotted the along-scan PSD for cutouts constrained to have:
  - $2.0 < T_{90} - T_{10} < 2.1K$ and
  - Log likelihood, determined by the ML algorithm (S2-ID-036) , > 194
- These constrains lead to spectra with about the same overall energy level

  Making it straightforward to compare them.

Our Approach

- As noted in S2-ID-036 we used 128$\times$128 pixel samples extracted from the L2 fields:
  - We refer to these approximately 128$\times$128 km^2 extractions as cutouts.
  - Cutouts were restricted to be:
    - $>$95% “clear",
    - Within 400 pixels of nadir, and
    - $<\approx$ 50% overlap
  - Resulted in $\approx$12 million cutouts.
- In an attempt to find what the ML algorithm was keying on, we examined cutout:
  - Temperature range
  - Variance
  - Along-scan and along-track structure functions and
  - Along-scan and along-track power spectral densities (PSD).
- With some intriguing results for the latter.
- Specifically, we plotted the along-scan PSD for cutouts constrained to have:
  - $2.0 < T_{90} - T_{10} < 2.1K$ and
  - Log likelihood, determined by the ML algorithm (S2-ID-036) , $>$ 194
- These constrains lead to spectra with about the same overall energy level

  Making it straightforward to compare them.

Our Approach

- As noted in S2-ID-036 we used 128×128 pixel samples extracted from the L2 fields:
  - We refer to these approximately 128×128 km^2 extractions as cutouts.
  - Cutouts were restricted to be:
    - $>$95% “clear",
    - Within 400 pixels of nadir, and
    - $<\approx$ 50% overlap
  - Resulted in $\approx$12 million cutouts.
- In an attempt to find what the ML algorithm was keying on, we examined cutout:
  - Temperature range
  - Variance
  - Along-scan and along-track structure functions and
  - Along-scan and along-track power spectral densities (PSD).
- With some intriguing results for the latter.
- Specifically, we plotted the along-scan PSD for cutouts constrained to have:
  - $2.0 < T_{90} - T_{10} < 2.1K$ and
  - Log likelihood, determined by the ML algorithm (S2-ID-036) , > 194
- These constrains lead to spectra with about the same overall energy level

  Making it straightforward to compare them.

Our Approach

- As noted in S2-ID-036 we used 128×128 pixel samples extracted from the L2 fields:
  - We refer to these approximately 128×128 km^2 extractions as cutouts.
  - Cutouts were restricted to be:
    - $>$95% "clear",
    - Within 400 pixels of nadir, and
    - $<\approx$ 50% overlap
  - Resulted in $\approx$12 million cutouts.
- In an attempt to find what the ML algorithm was keying on, we examined cutout:
  - Temperature range
  - Variance
  - Along-scan and along-track structure functions and
  - Along-scan and along-track power spectral densities (PSD).
- With some intriguing results for the latter.
- Specifically, we plotted the along-scan PSD for cutouts constrained to have:
  - $2.0 < T_{90} - T_{10} < 2.1K$ and
  - Log likelihood, determined by the ML algorithm (S2-ID-036) , > 194
- These constrains lead to spectra with about the same overall energy level

  Making it straightforward to compare them.

Our Approach

- As noted in S2-ID-036 we used 128×128 pixel samples extracted from the L2 fields:
  - We refer to these approximately 128×128 km^2 extractions as cutouts.
  - Cutouts were restricted to be:
    - $>$95% “clear",
    - Within 400 pixels of nadir, and
    - $<\approx$ 50% overlap
  - Resulted in $\approx$12 million cutouts.
- In an attempt to find what the ML algorithm was keying on, we examined cutout:
  - Temperature range
  - Variance
  - Along-scan and along-track structure functions and
  - Along-scan and along-track power spectral densities (PSD).
- With some intriguing results for the latter.
- Specifically, we plotted the along-scan PSD for cutouts constrained to have:
  - $2.0 < T_{90} - T_{10} < 2.1K$ and
  - Log likelihood, determined by the ML algorithm (S2-ID-036) , > 194
- These constrains lead to spectra with about the same overall energy level

  Making it straightforward to compare them.

Our Approach

- As noted in S2-ID-036 we used 128×128 pixel samples extracted from the L2 fields:
  - We refer to these approximately 128×128 km^2 extractions as cutouts.
  - Cutouts were restricted to be:
    - $>$95% "clear",
    - Within 400 pixels of nadir, and
    - $<\approx$ 50% overlap
  - Resulted in $\approx$12 million cutouts.
- In an attempt to find what the ML algorithm was keying on, we examined cutout:
  - Temperature range
  - Variance
  - Along-scan and along-track structure functions and
  - Along-scan and along-track power spectral densities (PSD).
- With some intriguing results for the latter.
- Specifically, we plotted the along-scan PSD for cutouts constrained to have:
  - $2.0 < T_{90} - T_{10} < 2.1K$ and
  - Log likelihood, determined by the ML algorithm (S2-ID-036) , > 194
- These constrains lead to spectra with about the same overall energy level

  Making it straightforward to compare them.

Our Approach

- As noted in S2-ID-036 we used 128×128 pixel samples extracted from the L2 fields:
  - We refer to these approximately 128×128 km^2 extractions as cutouts.
  - Cutouts were restricted to be:
    - $>$95% "clear",
    - Within 400 pixels of nadir, and
    - $<\approx$ 50% overlap
  - Resulted in $\approx$12 million cutouts.
- In an attempt to find what the ML algorithm was keying on, we examined cutout:
  - Temperature range
  - Variance
  - Along-scan and along-track structure functions and
  - Along-scan and along-track power spectral densities (PSD).
- With some intriguing results for the latter.
- Specifically, we plotted the along-scan PSD for cutouts constrained to have:
  - $2.0 < T_{90} - T_{10} < 2.1K$ and
  - Log likelihood, determined by the ML algorithm (S2-ID-036) , $>$ 194
- These constrains lead to spectra with about the same overall energy level

  Making it straightforward to compare them.

Our Approach

- As noted in S2-ID-036 we used 128×128 pixel samples extracted from the L2 fields:
  - We refer to these approximately 128×128 km^2 extractions as cutouts.
  - Cutouts were restricted to be:
    - $>$95% “clear",
    - Within 400 pixels of nadir, and
    - $<\approx$ 50% overlap
  - Resulted in ≈12 million cutouts.
- In an attempt to find what the ML algorithm was keying on, we examined cutout:
  - Temperature range
  - Variance
  - Along-scan and along-track structure functions and
  - Along-scan and along-track power spectral densities (PSD).
- With some intriguing results for the latter.
- Specifically, we plotted the along-scan PSD for cutouts constrained to have:
  - $2.0 < T_{90} - T_{10} < 2.1K$ and
  - Log likelihood, determined by the ML algorithm (S2-ID-036) , > 194
- These constrains lead to spectra with about the same overall energy level

  Making it straightforward to compare them.

The Result - Spectra as a Function of Latitude

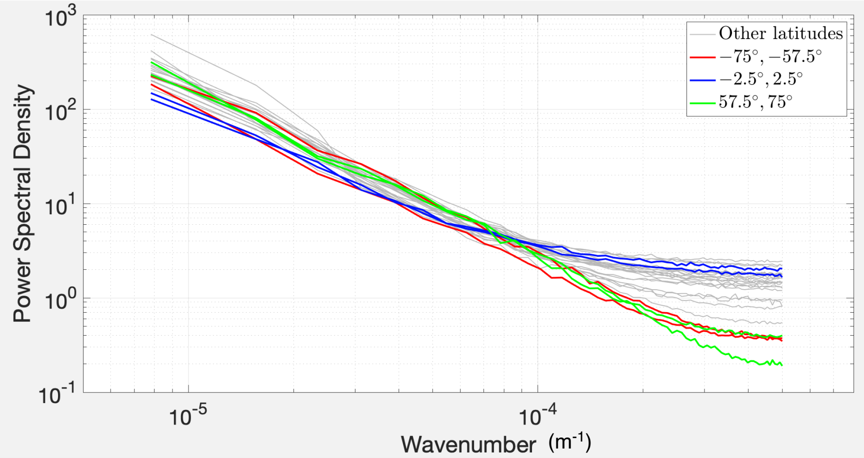

Low-latitude spectra level off at high energy levels.

High-latitude spectra level off at low energy levels.

Red for southern hemisphere 57.5° and 75°S

Green for northern hemisphere 57.5° and 75°N

The Result - Spectra as a Function of Latitude

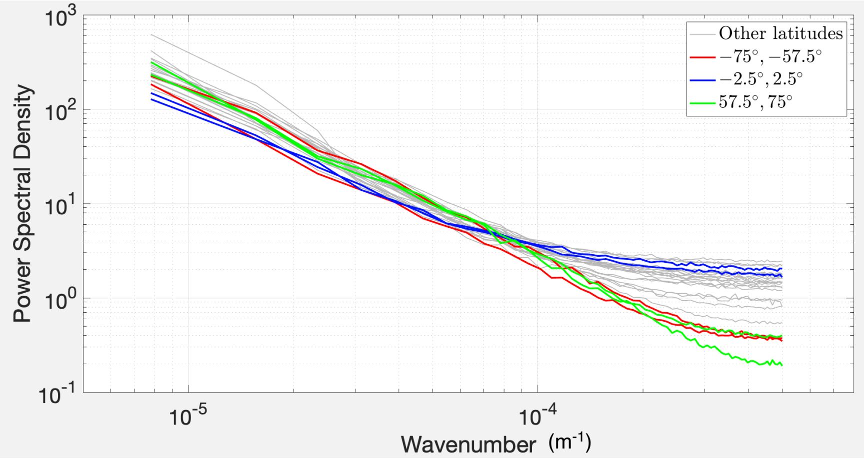

Low-latitude spectra level off at high energy levels.

High-latitude spectra level off at low energy levels.

Red for southern hemisphere 57.5° and 75° S

Green for northern hemisphere 57.5° and 75° N

The Result - Spectra as a Function of Latitude

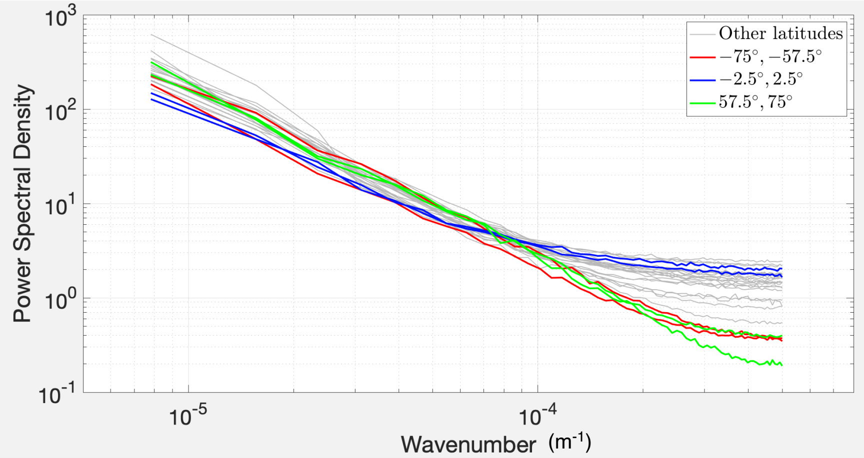

Low-latitude spectra level off at high energy levels.

High-latitude spectra level off at low energy levels.

Red for southern hemisphere 57.5° and 75° S

Green for northern hemisphere 57.5° and 75° N

More on the Odd Behavior: Instrument Noise?

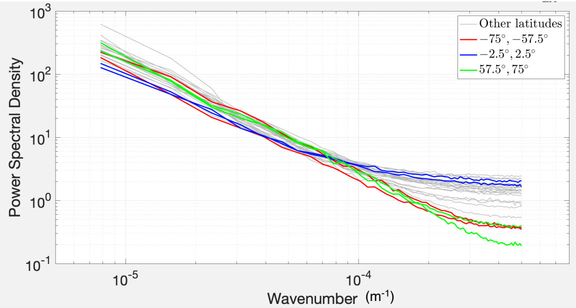

- Leveling off of spectra at high wavenumber is often associated with instrument noise.

  With the instrument noise defining the energy level at which the spectra level off.
- Assuming that the instrument noise is independent of space and time

  One would expect the floor of all spectra to be about the same,

  BUT, this is clearly not the case.
- So maybe there is a geophysical reason for the latitudinal dependence of the spectra.

More on the Odd Behavior: Instrument Noise?

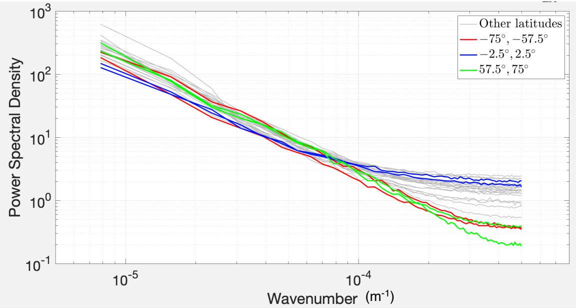

- Leveling off of spectra at high wavenumber is often associated with instrument noise.

  With the instrument noise defining the energy level at which the spectra level off.
- Assuming that the instrument noise is independent of space and time

  One would expect the floor of all spectra to be about the same,

  BUT, this is clearly not the case.
- So maybe there is a geophysical reason for the latitudinal dependence of the spectra.

More on the Odd Behavior: Instrument Noise?

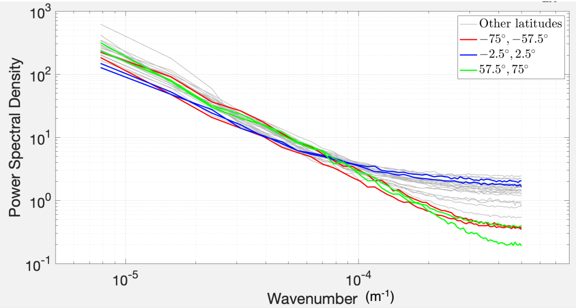

- Leveling off of spectra at high wavenumber is often associated with instrument noise.

  With the instrument noise defining the energy level at which the spectra level off.
- Assuming that the instrument noise is independent of space and time

  One would expect the floor of all spectra to be about the same,

  BUT, this is clearly not the case.
- So maybe there is a geophysical reason for the latitudinal dependence of the spectra.

More on the Odd Behavior: Instrument Noise?

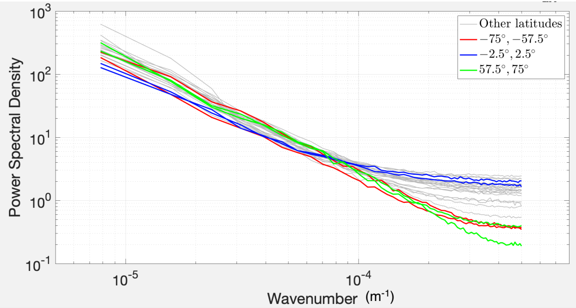

- Leveling off of spectra at high wavenumber is often associated with instrument noise.

  With the instrument noise defining the energy level at which the spectra level off.
- Assuming that the instrument noise is independent of space and time

  One would expect the floor of all spectra to be about the same,

  BUT, this is clearly not the case.
- So maybe there is a geophysical reason for the latitudinal dependence of the spectra.

More on the Odd Behavior: Instrument Noise?

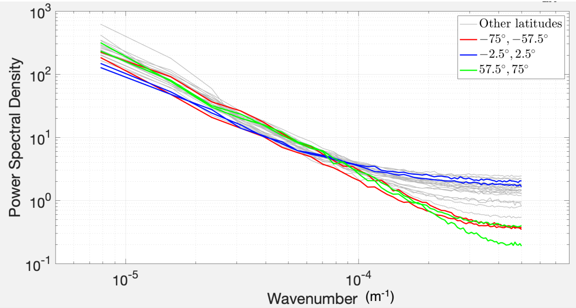

- Leveling off of spectra at high wavenumber is often associated with instrument noise.

  With the instrument noise defining the energy level at which the spectra level off.
- Assuming that the instrument noise is independent of space and time

  One would expect the floor of all spectra to be about the same,

  BUT, this is clearly not the case.
- So maybe there is a geophysical reason for the latitudinal dependence of the spectra.

More on the Odd Behavior: Instrument Noise?

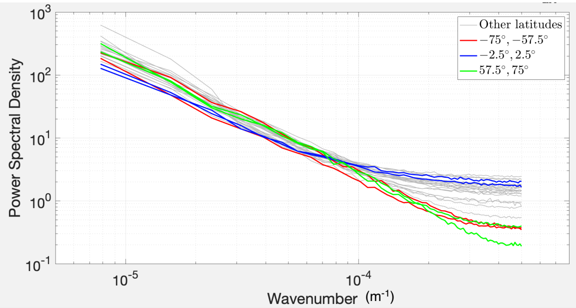

- Leveling off of spectra at high wavenumber is often associated with instrument noise.

  With the instrument noise defining the energy level at which the spectra level off.
- Assuming that the instrument noise is independent of space and time

  One would expect the floor of all spectra to be about the same,

  BUT, this is clearly not the case.
- So maybe there is a geophysical reason for the latitudinal dependence of the spectra.

More on the Odd Behavior: Geophysical?

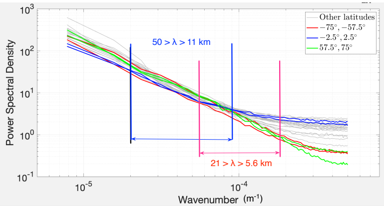

- Looking for a geophysical explanation, we determined slopes over two ranges:
  - mesoscale (11-50 km, blue) and
  - sub-mesoscale (5.6-21 km, red)
- And plotted these versus latitude.
  - Although ragged mesoscale slopes are independent of latitude, while
  - Sub-mesoscale slopes show a well defined ≈cosine dependence on latitude.
- We were excited and asked Jörn Callis to join our effort.
  - He could think of no reason for a latitudinal dependence.
  - Were we sure that it wasn't instrument related?
- So we dug deeper.

More on the Odd Behavior: Geophysical?

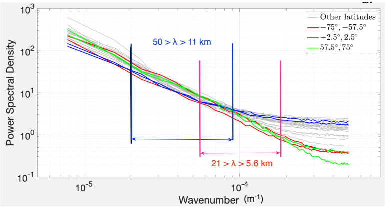

- Looking for a geophysical explanation, we determined slopes over two ranges:
  - mesoscale (11-50 km, blue) and
  - sub-mesoscale (5.6-21 km, red)
- And plotted these versus latitude.
  - Although ragged mesoscale slopes are independent of latitude, while
  - Sub-mesoscale slopes show a well defined ≈cosine dependence on latitude.
- We were excited and asked Jörn Callis to join our effort.
  - He could think of no reason for a latitudinal dependence.
  - Were we sure that it wasn't instrument related?
    -
    - But the daytime latitudinal dependence mimicked the nighttime dependence.
- So we dug deeper.

More on the Odd Behavior: Geophysical?

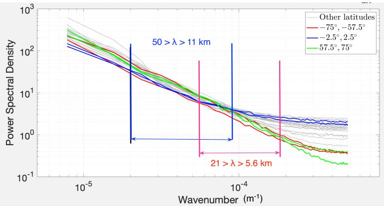

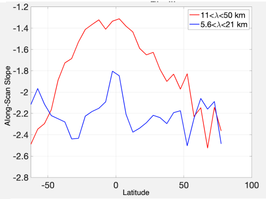

- Looking for a geophysical explanation, we determined slopes over two ranges:
  - mesoscale (11-50 km, blue) and
  - sub-mesoscale (5.6-21 km, red)
- And plotted these versus latitude.
  - Although ragged mesoscale slopes are independent of latitude, while
  - Sub-mesoscale slopes show a well defined ≈cosine dependence on latitude.
- We were excited and asked Jörn Callis to join our effort.
  - He could think of no reason for a latitudinal dependence.
  - Were we sure that it wasn't instrument related?
- So we dug deeper.

More on the Odd Behavior: Geophysical?

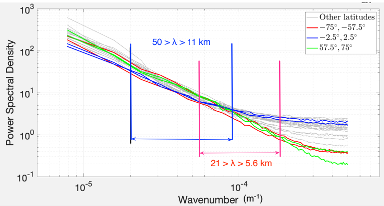

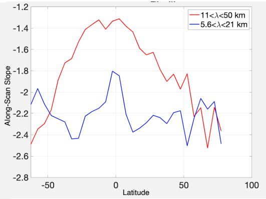

- Looking for a geophysical explanation, we determined slopes over two ranges:
  - mesoscale (11-50 km, blue) and
  - sub-mesoscale (5.6-21 km, red)
- And plotted these versus latitude.
  - Although ragged mesoscale slopes are independent of latitude, while
  - Sub-mesoscale slopes show a well defined ≈cosine dependence on latitude.
- We were excited and asked Jörn Callis to join our effort.
  - He could think of no reason for a latitudinal dependence.
  - Were we sure that it wasn't instrument related?
- So we dug deeper.

More on the Odd Behavior: Geophysical?

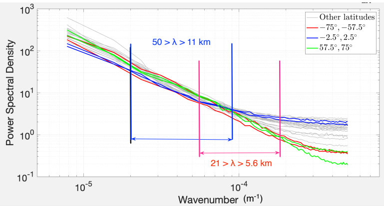

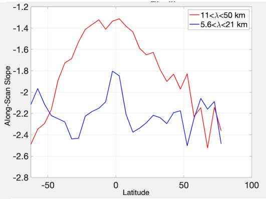

- Looking for a geophysical explanation, we determined slopes over two ranges:
  - mesoscale (11-50 km, blue) and
  - sub-mesoscale (5.6-21 km, red)
- And plotted these versus latitude.
  - Although ragged mesoscale slopes are independent of latitude, while
  - Sub-mesoscale slopes show a well defined ≈cosine dependence on latitude.
- We were excited and asked Jörn Callis to join our effort.
  - He could think of no reason for a latitudinal dependence.
  - Were we sure that it wasn't instrument related?
- So we dug deeper.

More on the Odd Behavior: Geophysical?

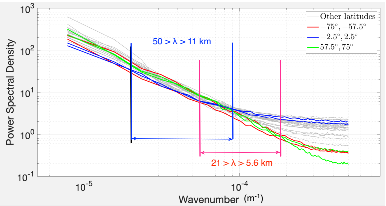

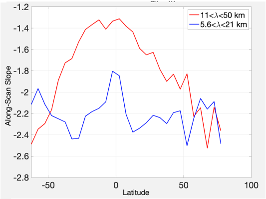

- Looking for a geophysical explanation, we determined slopes over two ranges:
  - mesoscale (11-50 km, blue) and
  - sub-mesoscale (5.6-21 km, red)
- And plotted these versus latitude.
  - Although ragged mesoscale slopes are independent of latitude, while
  - Sub-mesoscale slopes show a well defined ≈cosine dependence on latitude.
    Is this indicative of a new sub-mesoscale behavior, possibly depending on Coriolis?
- We were excited and asked Jörn Callis to join our effort.
  - He could think of no reason for a latitudinal dependence.
  - Were we sure that it wasn't instrument related?
- So we dug deeper.

More on the Odd Behavior: Geophysical?

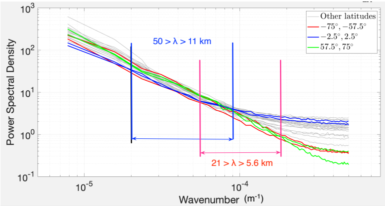

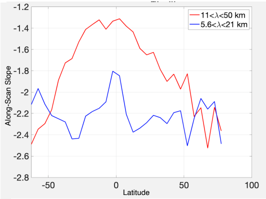

- Looking for a geophysical explanation, we determined slopes over two ranges:
  - mesoscale (11-50 km, blue) and
  - sub-mesoscale (5.6-21 km, red)
- And plotted these versus latitude.
  - Although ragged mesoscale slopes are independent of latitude, while
  - Sub-mesoscale slopes show a well defined ≈cosine dependence on latitude.

    Is this indicative of a new sub-mesoscale behavior, possibly depending on Coriolis?
- We were excited and asked Jörn Callis to join our effort.
  - He could think of no reason for a latitudinal dependence.
  - Were we sure that it wasn't instrument related?
    - But the daytime latitudinal dependence mimicked the nighttime dependence.
- So we dug deeper.

More on the Odd Behavior: Geophysical?

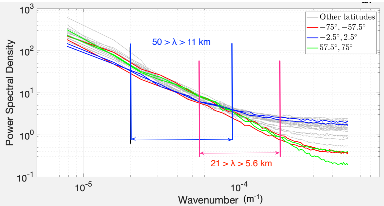

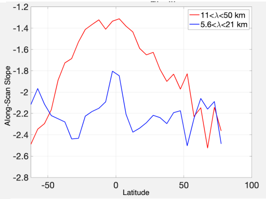

- Looking for a geophysical explanation, we determined slopes over two ranges:
  - mesoscale (11-50 km, blue) and
  - sub-mesoscale (5.6-21 km, red)
- And plotted these versus latitude.
  - Although ragged mesoscale slopes are independent of latitude, while
  - Sub-mesoscale slopes show a well defined ≈cosine dependence on latitude.

    ~~Is this indicative of a new sub-mesoscale behavior, possibly depending on Coriolis?~~
- We were excited and asked Jörn Callis to join our effort.
  - He could think of no reason for a latitudinal dependence.
  - Were we sure that it wasn't instrument related?
    - But the daytime latitudinal dependence mimicked the nighttime dependence.
- So we dug deeper.

More on the Odd Behavior: Geophysical?

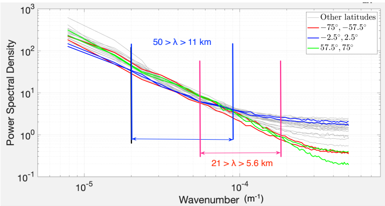

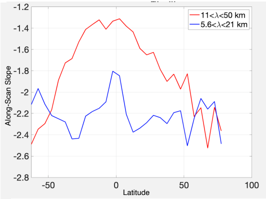

- Looking for a geophysical explanation, we determined slopes over two ranges:
  - mesoscale (11-50 km, blue) and
  - sub-mesoscale (5.6-21 km, red)
- And plotted these versus latitude.
  - Although ragged mesoscale slopes are independent of latitude, while
  - Sub-mesoscale slopes show a well defined ≈cosine dependence on latitude.

  ~~Is this indicative of a new sub-mesoscale behavior, possibly depending on Coriolis?~~
- We were excited and asked Jörn Callis to join our effort.
  - He could think of no reason for a latitudinal dependence.
  - Were we sure that it wasn't instrument related?
    -
    - But the daytime latitudinal dependence mimicked the nighttime dependence.
- So we dug deeper.

More on the Odd Behavior: Geophysical?

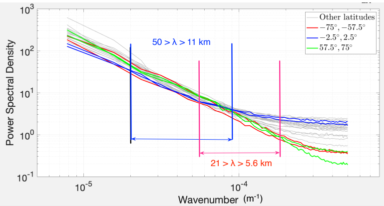

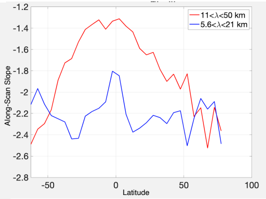

- Looking for a geophysical explanation, we determined slopes over two ranges:
  - mesoscale (11-50 km, blue) and
  - sub-mesoscale (5.6-21 km, red)
- And plotted these versus latitude.
  - Although ragged mesoscale slopes are independent of latitude, while
  - Sub-mesoscale slopes show a well defined ≈cosine dependence on latitude.

    ~~Is this indicative of a new sub-mesoscale behavior, possibly depending on Coriolis?~~
- We were excited and asked Jörn Callis to join our effort.
  - He could think of no reason for a latitudinal dependence.
  - Were we sure that it wasn't instrument related?
    - Maybe cooling (warming) of MODIS as it moves into (out of) Earth's shadow?
    - But the daytime latitudinal dependence mimicked the nighttime dependence.
- So we dug deeper.

More on the Odd Behavior: Geophysical?

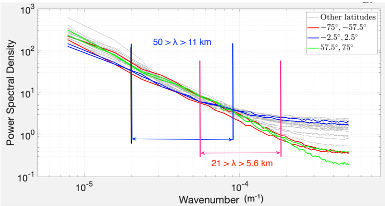

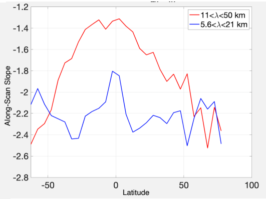

- Looking for a geophysical explanation, we determined slopes over two ranges:
  - mesoscale (11-50 km, blue) and
  - sub-mesoscale (5.6-21 km, red)
- And plotted these versus latitude.
  - Although ragged mesoscale slopes are independent of latitude, while
  - Sub-mesoscale slopes show a well defined ≈cosine dependence on latitude.

    ~~Is this indicative of a new sub-mesoscale behavior, possibly depending on Coriolis?~~
- We were excited and asked Jörn Callis to join our effort.
  - He could think of no reason for a latitudinal dependence.
  - Were we sure that it wasn't instrument related?
    - ~~Maybe cooling (warming) of MODIS as it moves into (out of) Earth's shadow?~~
    - But the daytime latitudinal dependence mimicked the nighttime dependence.
- So we dug deeper.

More on the Odd Behavior: Geophysical?

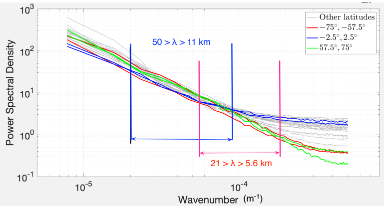

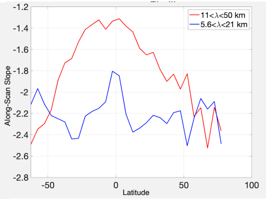

- Looking for a geophysical explanation, we determined slopes over two ranges:
  - mesoscale (11-50 km, blue) and
  - sub-mesoscale (5.6-21 km, red)
- And plotted these versus latitude.
  - Although ragged mesoscale slopes are independent of latitude, while
  - Sub-mesoscale slopes show a well defined ≈cosine dependence on latitude.

    ~~Is this indicative of a new sub-mesoscale behavior, possibly depending on Coriolis?~~
- We were excited and asked Jörn Callis to join our effort.
  - He could think of no reason for a latitudinal dependence.
  - Were we sure that it wasn't instrument related?
    - ~~Maybe cooling (warming) of MODIS as it moves into (out of) Earth's shadow?~~
    - But the daytime latitudinal dependence mimicked the nighttime dependence.
- So we dug deeper.

Outline

Structure Function Estimation of Precision in SST Observations

- Along-scan and along-track variograms were determined from all cutouts falling within each element of a $200\,\mathrm{km} \times 200\,\mathrm{km} \times 5\,\mathrm{day}$ non-overlapping global grid.
- The precision of SST retrievals was determined from these variograms based on an alternative to Wu et al. (2017):
  - A 4^{th} order polynomial was fit to the square root of the variogram for separations < 20 km
  - And extrapolated to zero to obtain an estimate of instrument noise - σ.

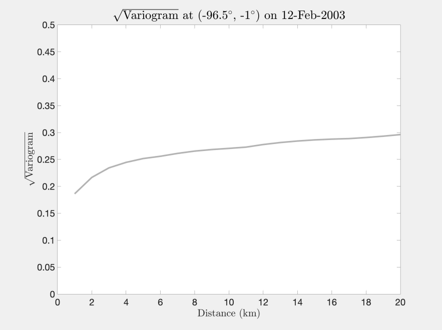

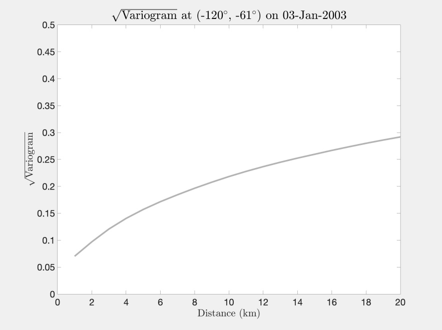

Wu, F.; Cornillon, P.; Boussidi, B.; Guan, L . *Determining the Pixel-to-Pixel Uncertainty in Satellite-Derived SST Fields.* Remote Sens. 2017, 9(9), 877; https://doi.org/10.3390/rs9090877

Structure Function Estimation of Precision in SST Observations

- Along-scan and along-track variograms were determined from all cutouts falling within each element of a $200\,\mathrm{km} \times 200\,\mathrm{km} \times 5\,\mathrm{day}$ non-overlapping global grid.
- The precision of SST retrievals was determined from these variograms based on an alternative to Wu et al. (2017):
  - A 4^{th} order polynomial was fit to the square root of the variogram for separations < 20 km
  - And extrapolated to zero to obtain an estimate of instrument noise - σ.

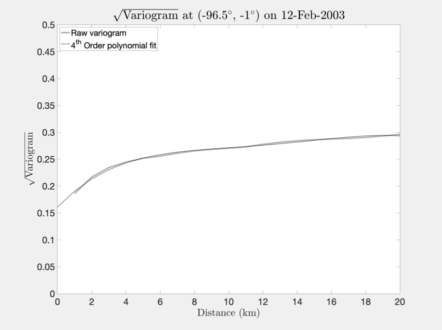

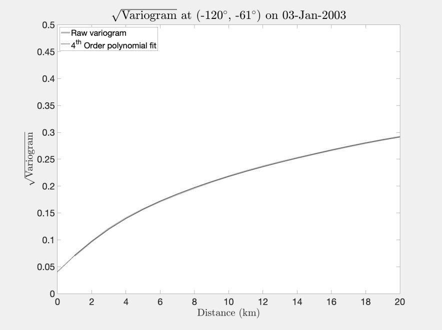

Wu, F.; Cornillon, P.; Boussidi, B.; Guan, L . *Determining the Pixel-to-Pixel Uncertainty in Satellite-Derived SST Fields*. Remote Sens. 2017, 9(9), 877; https://doi.org/10.3390/rs9090877

Structure Function Estimation of Precision in SST Observations

- Along-scan and along-track variograms were determined from all cutouts falling within each element of a 200 km $\times$ 200 km $\times$ 5 day non-overlapping global grid.
- The precision of SST retrievals was determined from these variograms based on an alternative to Wu et al. (2017):
  - A 4^{th} order polynomial was fit to the square root of the variogram for separations $<$ 20 km
  - And extrapolated to zero to obtain an estimate of instrument noise - σ.

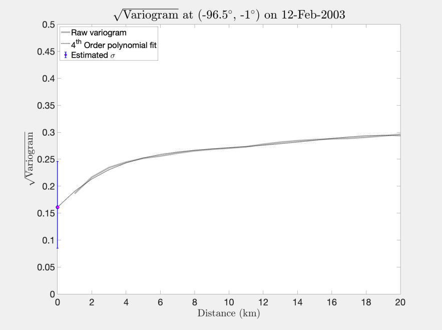

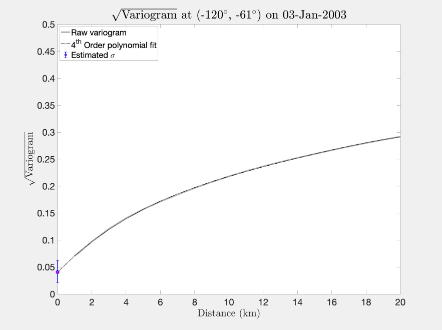

Wu, F.; Cornillon, P.; Boussidi, B.; Guan, L . *Determining the Pixel-to-Pixel Uncertainty in Satellite-Derived SST Fields*. Remote Sens. 2017, 9(9), 877; https://doi.org/10.3390/rs9090877

Geographic Distribution of Along-Scan σ

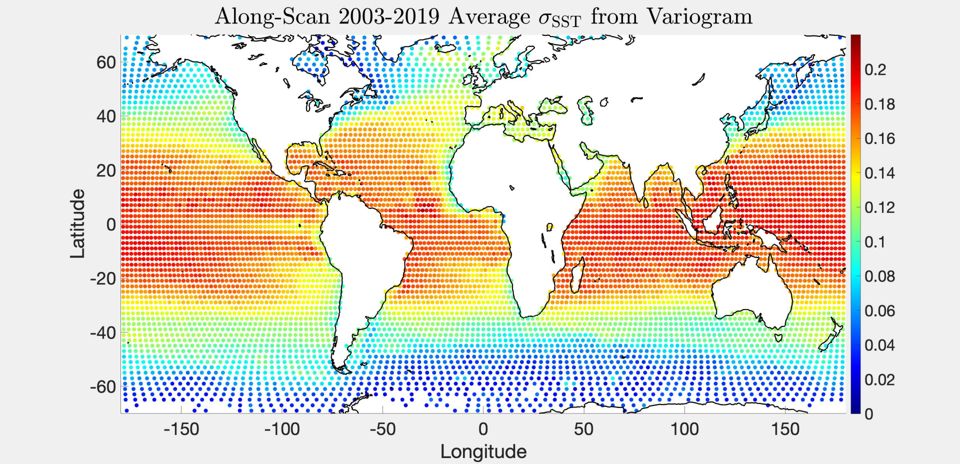

Temperature Dependence

- An alternative to a latitudinal dependence for sigma is a temperature dependence.
- So we scatter plotted σ vs $\overline{SST}$. Two things to note:
  - A well defined linear dependence of σ on mean SST
  - And a low σ region for mean SST above about 22°.

Temperature Dependence

- An alternative to a latitudinal dependence for sigma is a temperature dependence.
- So we scatter plotted σ vs $\overline{SST}$. Two things to note:
  - A well defined linear dependence of σ on mean SST
  - And a low σ region for mean SST above about 22°.

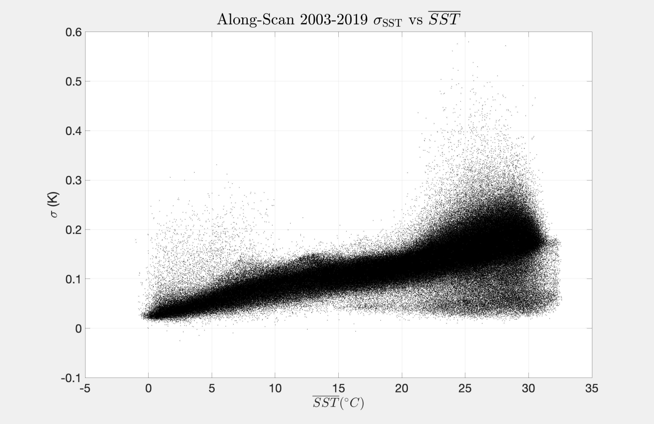

Temperature Dependence

- An alternative to a latitudinal dependence for sigma is a temperature dependence.
- So we scatter plotted σ vs $\overline{SST}$. Two things to note:
  - A well defined linear dependence of σ on mean SST
  - And a low σ region for mean SST above about 22°.

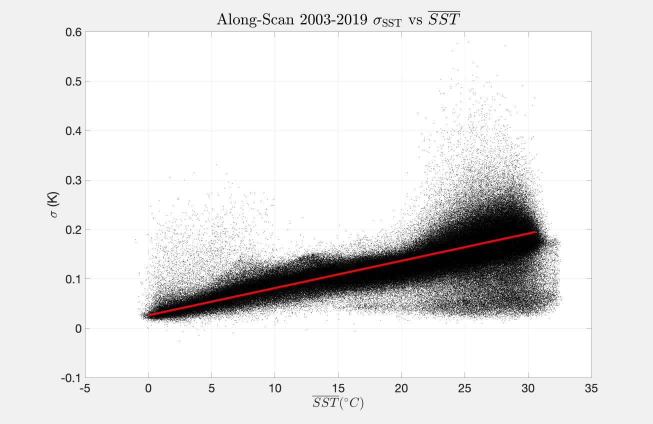

Temperature Dependence

- An alternative to a latitudinal dependence for sigma is a temperature dependence.
- So we scatter plotted σ vs $\overline{SST}$. Two things to note:
  - A well defined linear dependence of σ on mean SST
  - And a low σ region for mean SST above about 22°.

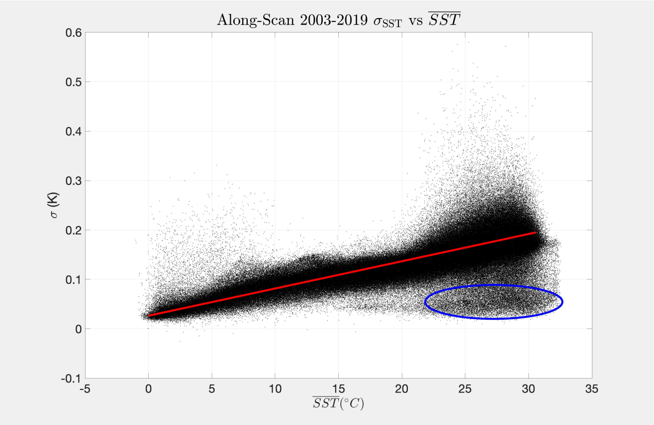

Temperature Dependence - Consider the 2d histogram of σ vs $\overline{SST}$

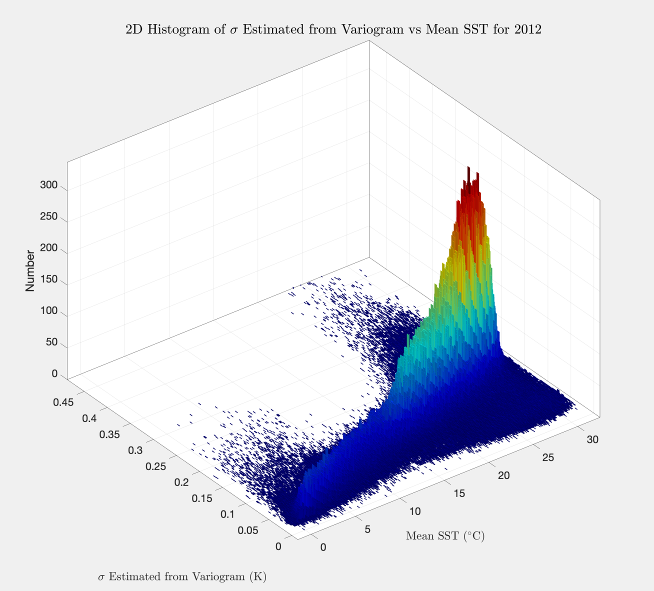

Temperature Dependence - Consider the 2d histogram of σ vs $\overline{SST}$

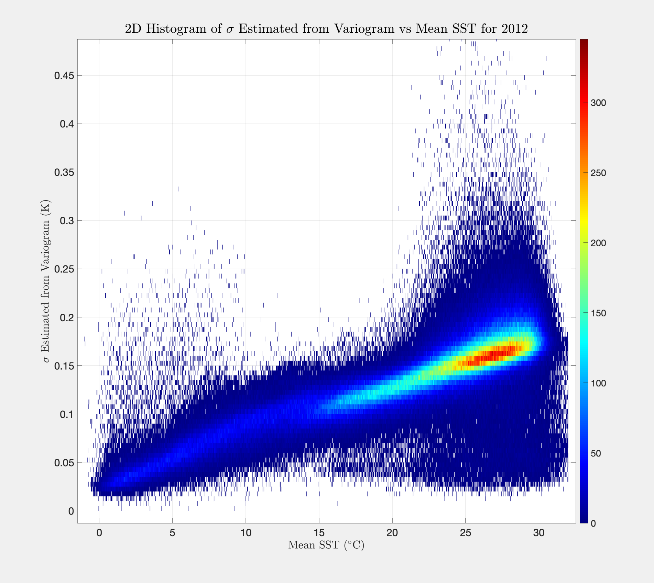

Temperature Dependence - $\sigma = 0.031 + 0.0048 \times \overline{SST}$

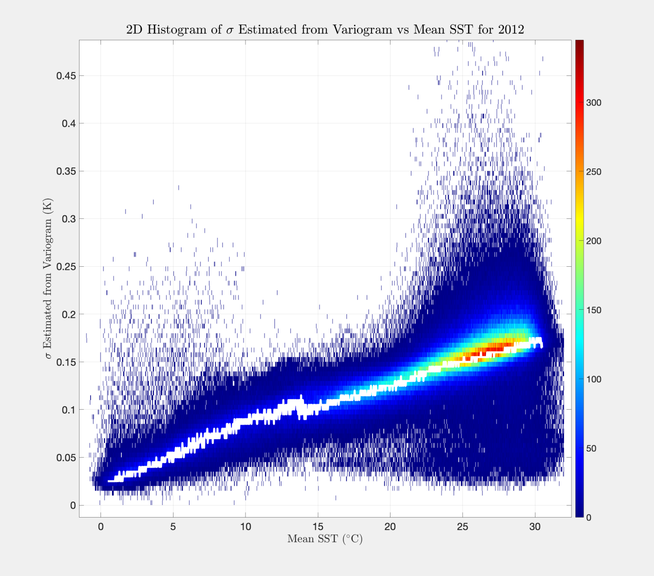

Temperature Dependence - $\sigma = 0.031 + 0.0048 \times \overline{\mathrm{SST}}$

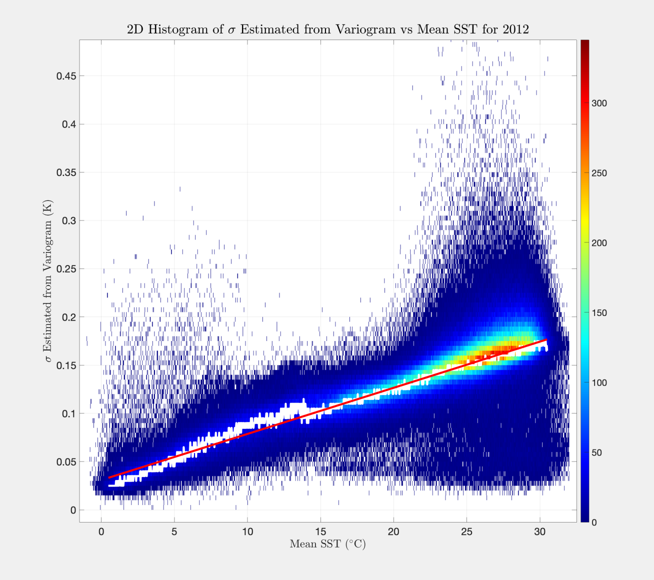

Temperature Dependence - Geographic Location of $\downarrow \sigma$ for $\uparrow \overline{\text{SST}}$

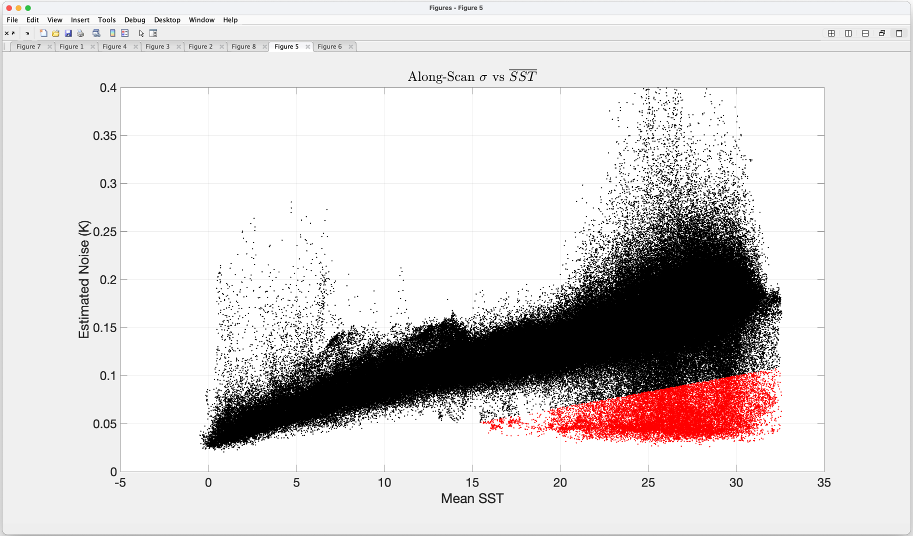

Temperature Dependence - Geographic Location of $\downarrow \sigma$ for $\uparrow \overline{\text{SST}}$

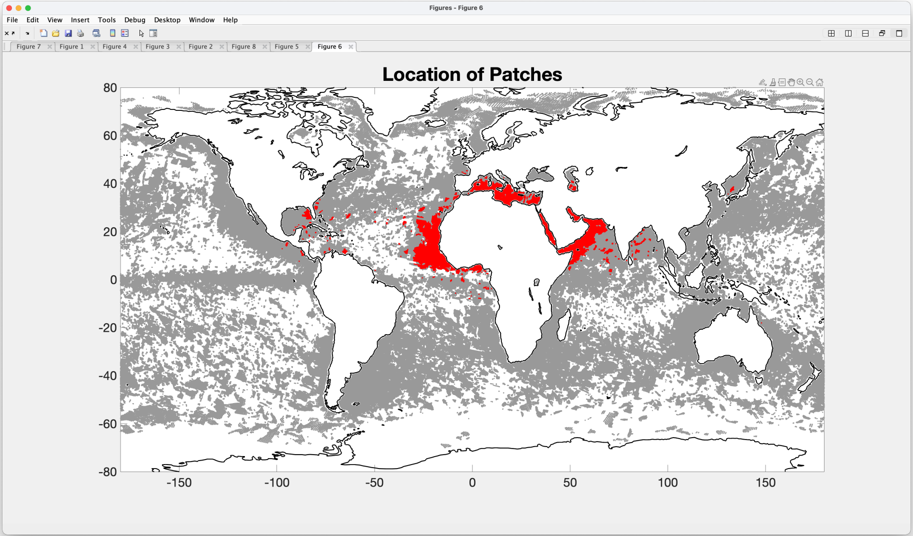

Outline

1. Motivation
2. Problem Resolved - Sort of
3. Conclusions

Conclusions

- There appears to be a strong dependence of MODIS L2 σ on $\overline{\mathrm{SST}}$.
  - $\sigma = 0.031 + 0.0048 \times \overline{\mathrm{SST}}$
  - With $\sigma \approx 0.03K$ at $0^\circ C$ and $\sigma \approx 0.18K$ at $30^\circ C$
  - Data shown are for along-scan σ but along-track σ also increase with $\overline{\mathrm{SST}}$
- The region around equatorial Africa is anomalous wtih low σ for $\overline{\mathrm{SST}} > 22^\circ$C
- We have not shown that this is instrument noise; it could be
  - A processing issue
  - And or related to the misclassification of clouds.
- Whatever it is, it is a problem for those interested in small scale features.

Conclusions

- There appears to be a strong dependence of MODIS L2 σ on $\overline{\mathrm{SST}}$.
  - $\sigma = 0.031 + 0.0048 \times \overline{\mathrm{SST}}$
  - With $\sigma \approx 0.03K$ at $0^\circ C$ and $\sigma \approx 0.18K$ at $30^\circ C$
  - Data shown are for along-scan σ but along-track σ also increase with $\overline{\mathrm{SST}}$
- The region around equatorial Africa is anomalous wtih low σ for $\overline{\mathrm{SST}} > 22^\circ\mathrm{C}$
- We have not shown that this is instrument noise; it could be
  - A processing issue
  - And or related to the misclassification of clouds.
- Whatever it is, it is a problem for those interested in small scale features.

Conclusions

- There appears to be a strong dependence of MODIS L2 σ on $\overline{\mathrm{SST}}$.
  - $\sigma = 0.031 + 0.0048 \times \overline{\mathrm{SST}}$
  - With $\sigma \approx 0.03K$ at $0^\circ C$ and $\sigma \approx 0.18K$ at $30^\circ C$
  - Data shown are for along-scan σ but along-track σ also increase with $\overline{\mathrm{SST}}$
- The region around equatorial Africa is anomalous wtih low σ for $\overline{\mathrm{SST}} > 22^\circ\mathrm{C}$
- We have not shown that this is instrument noise; it could be
  - A processing issue
  - And or related to the misclassification of clouds.
- Whatever it is, it is a problem for those interested in small scale features.

Conclusions

- There appears to be a strong dependence of MODIS L2 σ on $\overline{\mathrm{SST}}$.
  - $\sigma = 0.031 + 0.0048 \times \overline{\mathrm{SST}}$
  - With $\sigma \approx 0.03K$ at $0^\circ C$ and $\sigma \approx 0.18K$ at $30^\circ C$
  - Data shown are for along-scan σ but along-track σ also increase with $\overline{\mathrm{SST}}$
- The region around equatorial Africa is anomalous wtih low σ for $\overline{\mathrm{SST}} > 22^\circ\mathrm{C}$
- We have not shown that this is instrument noise; it could be
  - A processing issue
  - And or related to the misclassification of clouds.
- Whatever it is, it is a problem for those interested in small scale features.

Conclusions

- There appears to be a strong dependence of MODIS L2 σ on $\overline{\mathrm{SST}}$.
  - $\sigma = 0.031 + 0.0048 \times \overline{\mathrm{SST}}$
  - With $\sigma \approx 0.03K$ at $0^{\circ}C$ and $\sigma \approx 0.18K$ at $30^{\circ}C$
  - Data shown are for along-scan σ but along-track σ also increase with $\overline{\mathrm{SST}}$
- The region around equatorial Africa is anomalous wtih low σ for $\overline{\mathrm{SST}} > 22^{\circ}$C
- We have not shown that this is instrument noise; it could be
  - A processing issue
  - And or related to the misclassification of clouds.
- Whatever it is, it is a problem for those interested in small scale features.

Conclusions

- There appears to be a strong dependence of MODIS L2 σ on $\overline{\mathrm{SST}}$.
  - $\sigma = 0.031 + 0.0048 \times \overline{\mathrm{SST}}$
  - With $\sigma \approx 0.03K$ at $0^\circ C$ and $\sigma \approx 0.18K$ at $30^\circ C$
  - Data shown are for along-scan σ but along-track σ also increase with $\overline{\mathrm{SST}}$
- The region around equatorial Africa is anomalous wtih low σ for $\overline{\mathrm{SST}} > 22^\circ$C
- We have not shown that this is instrument noise; it could be
  - A processing issue
  - And or related to the misclassification of clouds.
- Whatever it is, it is a problem for those interested in small scale features.

Conclusions

- There appears to be a strong dependence of MODIS L2 σ on $\overline{\mathrm{SST}}$.
  - $\sigma = 0.031 + 0.0048 \times \overline{\mathrm{SST}}$
  - With $\sigma \approx 0.03K$ at $0^\circ C$ and $\sigma \approx 0.18K$ at $30^\circ C$
  - Data shown are for along-scan σ but along-track σ also increase with $\overline{\mathrm{SST}}$
- The region around equatorial Africa is anomalous wtih low σ for $\overline{\mathrm{SST}} > 22^\circ$C
- We have not shown that this is instrument noise; it could be
  - A processing issue
  - And or related to the misclassification of clouds.
- Whatever it is, it is a problem for those interested in small scale features.

Conclusions

- There appears to be a strong dependence of MODIS L2 σ on $\overline{\mathrm{SST}}$.
  - $\sigma = 0.031 + 0.0048 \times \overline{\mathrm{SST}}$
  - With $\sigma \approx 0.03K$ at $0^\circ C$ and $\sigma \approx 0.18K$ at $30^\circ C$
  - Data shown are for along-scan σ but along-track σ also increase with $\overline{\mathrm{SST}}$
- The region around equatorial Africa is anomalous wtih low σ for $\overline{\mathrm{SST}} > 22^\circ$C
- We have not shown that this is instrument noise; it could be
  - A processing issue
  - And or related to the misclassification of clouds.
- Whatever it is, it is a problem for those interested in small scale features.

Conclusions

- There appears to be a strong dependence of MODIS L2 σ on $\overline{\mathrm{SST}}$.
  - $\sigma = 0.031 + 0.0048 \times \overline{\mathrm{SST}}$
  - With $\sigma \approx 0.03K$ at $0^\circ C$ and $\sigma \approx 0.18K$ at $30^\circ C$
  - Data shown are for along-scan σ but along-track σ also increase with $\overline{\mathrm{SST}}$
- The region around equatorial Africa is anomalous wtih low σ for $\overline{\mathrm{SST}} > 22^\circ$C
- We have not shown that this is instrument noise; it could be
  - A processing issue
  - And or related to the misclassification of clouds.
- Whatever it is, it is a problem for those interested in small scale features.